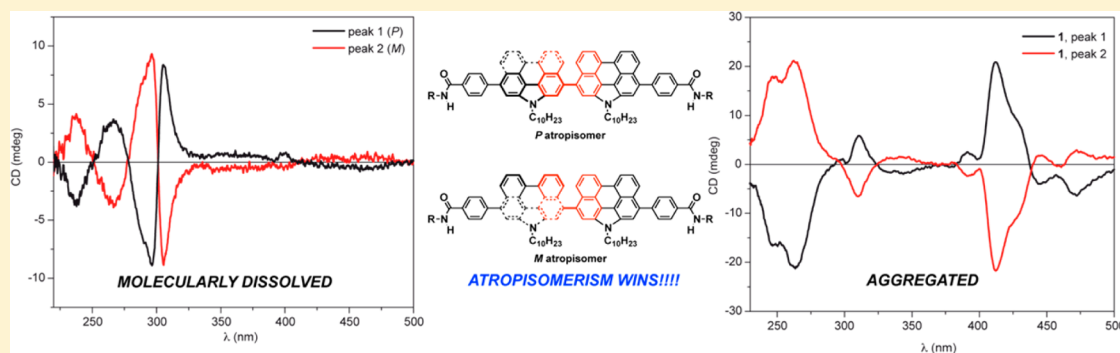


Influence of Axial and Point Chirality in the Chiral Self-Assembly of Twin *N*-Annulated Perylenecarboxamides

Julia Buendía,[†] Elisa E. Greciano,[†] and Luis Sánchez*[‡]

Departamento de Química Orgánica I, Facultad de Ciencias Químicas, Universidad Complutense de Madrid, 28040 Madrid, Spain

S Supporting Information



ABSTRACT: The synthesis of three bis(*N*-annulated perylenecarboxamides) endowed with achiral or chiral side chains is reported. The restricted rotation of the perylene moieties yields atropisomers that can be separated by chiral HPLC. The CD spectra of the six stereoisomers show a dichroic pattern in a good solvent that changes drastically upon adding a poor solvent that favors the aggregation. The cooperative character of the supramolecular polymerization mechanism of 1–3 has been determined by denaturation experiments, which reveal that the formation of homochiral aggregates is favored over the formation of heterochiral aggregates. A complete set of amplification of chirality experiments have been carried out, revealing the preponderance of axial chirality over point chirality. The results presented herein shed relevant light on the structural conditions exhibited by molecular units endowed with different elements of asymmetry to generate chiral supramolecular structures and the supremacy of axial chirality over point chirality in the origin of homochirality.

INTRODUCTION

Chirality is a topic that fascinates scientists of disciplines as different as chemistry, mathematics, biology, and geology.¹ The term *chirality* describes the structural property of an object that is nonsuperimposable on its mirror image. On a molecular level, chirality can be achieved by the presence of (a) stereogenic centers, (b) chiral planes, (c) chiral axes, or (d) helical chirality. Chiral structures have been reported to find applicability in different research areas such as asymmetric chemical synthesis and catalysis,² liquid crystals,³ conductive materials,⁴ chiral recognition,⁵ and, very importantly, determination of the origin of homochirality.⁶ These chiral supramolecular structures are generated by the noncovalent interaction of chiral molecular units that stack into aggregates in a process known as supramolecular polymerization.⁷ In a large number of the examples of chiral supramolecular polymers, the stereochemical information comes from the stereogenic centers located at the peripheral side chains decorating an aromatic nucleus that favors the columnar stacking.⁶ In these chiral supramolecular polymers, the handedness of the whole aggregate can be biased by only one stereogenic center per constitutive molecule.⁸ Benzene tricarboxamides,⁹ perylene bismides (PDIs),¹⁰ hexa-*peri*-hexabenzocoronenes,¹¹ and linear¹² or radial⁹ oligo(phenylene

ethynylenes) exemplify this effect of chiral transmission from point chirality to a helical supramolecular polymer. Interestingly, the influence of some other elements of molecular asymmetry in the transmission and amplification of chirality phenomena from the molecular to the supramolecular level has been also reported.^{13,14} However, in these reports, the prevalence of one type of asymmetry over the other has not been investigated.

To study the chirality of supramolecular polymers formed by units endowed with one or two elements of asymmetry (axial or axial plus point chirality) as well as to investigate the amplification of chirality phenomena by using atropisomers, we report herein on the synthesis of three twin *N*-annulated perylenecarboxamides (BNPCs; 1–3 in Figure 1). These π -conjugated platforms are being amply utilized in the field of organic electronics due to their highly anisotropic electronic properties.^{15,16} We have recently demonstrated that an *N*-annulated perylenedicarboxamide (NPDC) self-assembles efficiently to form highly emissive stable gels.¹⁷

The BNPC system possesses a binaphthalene moiety (red trace in compounds 1–3) that originates the *M* and *P*

Received: October 5, 2015

Published: November 19, 2015

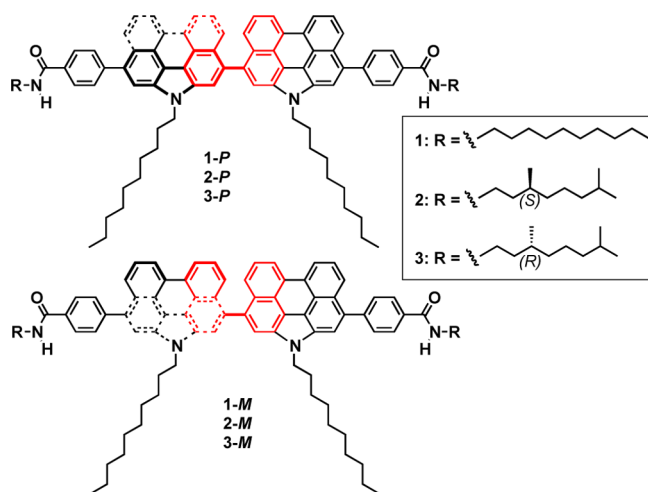


Figure 1. Chemical structures of the atropisomers 1–3.

atropisomers by the restricted rotation of the two *N*-annulated perylenecarboxamide (NPC) units. In addition, the decoration of the NPC moieties with chiral side chains gives access to the four possible (*M,S,S*), (*P,S,S*), (*M,R,R*), and (*P,R,R*) diastereomers. The separation of all the stereoisomers of 1–3 has allowed performing a detailed study on the chiroptical features of these systems in both molecularly dissolved and aggregated states. The cooperative supramolecular polymerization mechanism of 1–3 has been investigated by using the unfolding method reported by de Greef and Meijer.¹⁸ This method allows determining a complete set of thermodynamic parameters without heating the sample, thus avoiding the possible racemization of the atropisomers. The favored formation of homochiral aggregates is inferred from the derived values of the elongation binding constants, which strongly condition the results of the amplification of chirality experiments. These experiments, performed by mixing enantiomers and/or

diastereomers, further corroborate the supremacy of the axial chirality over the point chirality. The results presented in this paper contribute to increase the understanding of the structural rules regulating the chiral supramolecular organization of discrete molecules that finally yields complex chiral structures and the enormous utility of the thermodynamic data to justify the experimental results.

RESULTS AND DISCUSSION

Synthesis and Dichroic Characterization of the Diastereomers.

The synthesis of BNPCs 1–3 was achieved by following a multistep synthetic protocol by using perylene as the starting material (Figure 2). Following a previously reported method, the *N*-annulated perylene moiety 6 was prepared by successive nitration, cyclization with $P(OEt)_3$, and *N*-alkylation reactions.¹⁹ Treatment of 6 with 1 equiv of NBS affords compound 7, which is further reacted with the corresponding (4-(alkylcarbamoyl)phenyl)boronic acid 9 by a C–C cross-coupling Suzuki reaction catalyzed by palladium. The (4-(alkylcarbamoyl)phenyl)boronic acids 9 were prepared from the condensation reaction of the corresponding decylamine (8a), (*S*)-3,7-dimethyloctan-1-amine (8b), or (*R*)-3,7-dimethyl-octan-1-amine (8c) with 4-carboxyphenyl boronic acid in the presence of 1-ethyl-3-(3-(dimethylamino)propyl)-carbodiimide hydrochloride (EDC) and 4-dimethylaminopyridine (DMAP) as activating agents. Finally, the oxidative coupling of the NPC unit 10 with scandium triflate and 2,3-dichloro-5,6-dicyano-*p*-benzoquinone (DDQ) yields the BNPCs 1–3 in 38, 45, and 42% yields, respectively.^{17,20} This oxidative coupling generates the formation of the BNPC core in which the two *N*-annulated perylene moieties cannot freely rotate around the new aryl–aryl single bond, thus generating two enantiomers for 1 and two diastereomers for 2 and 3. In addition, since none of the faces is favored over the other, an equimolecular mixture of the possible stereoisomers should appear in the reaction.

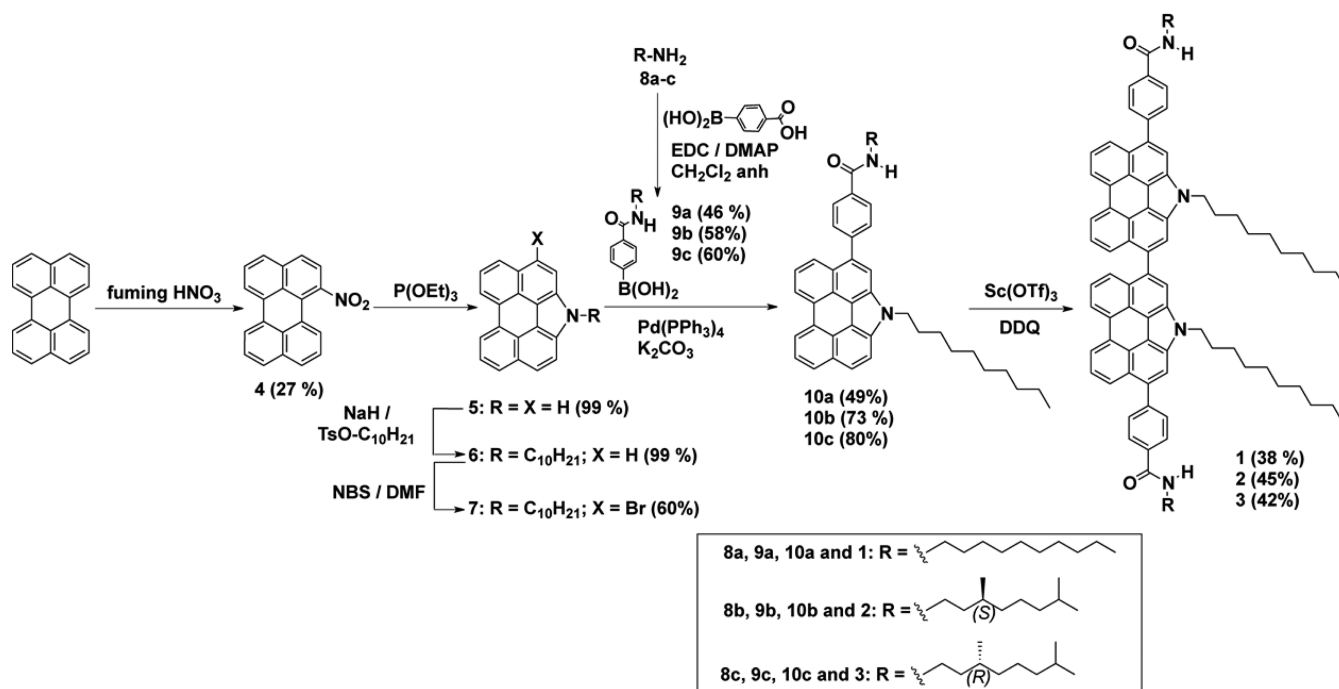


Figure 2. Synthesis of atropisomers 1–3.

The chemical structures of all new reported compounds have been confirmed by using NMR, FT-IR, and UV-vis spectroscopy, as well as HRMS analyses (see the [Supporting Information](#)). The ^1H NMR spectra of all three BNPCs 1–3 show a number of aromatic resonances corresponding to the BNPC core. Among them, two doublets at $\delta \sim 8.7$, corresponding to the two anisochronous protons at the bay positions of the perylene moiety, and also one triplet at $\delta \sim 7.6$, ascribable to the protons next to these bay positions, are clearly visible. Two triplets at $\delta \sim 6.4$ and at $\delta \sim 4.6$, corresponding to the amide N–H and to the $-\text{CH}_2-$ joint to the *N*-annulated ring, also confirm the structure of the proposed BNPCs. However, in the BNPCs 2 and 3 there is only one set of resonances, despite the fact that they should consist of an equimolecular mixture of two diastereomers each. The large separation between the two elements of symmetry, the point stereogenic center at the side chains and the hindered rotation of both NPC units, could reasonably explain that all of the protons of the four diastereomers (*M*,*S,S*), (*P*,*S,S*), (*M*,*R,R*), and (*P*,*R,R*) present the same chemical and magnetic environment.

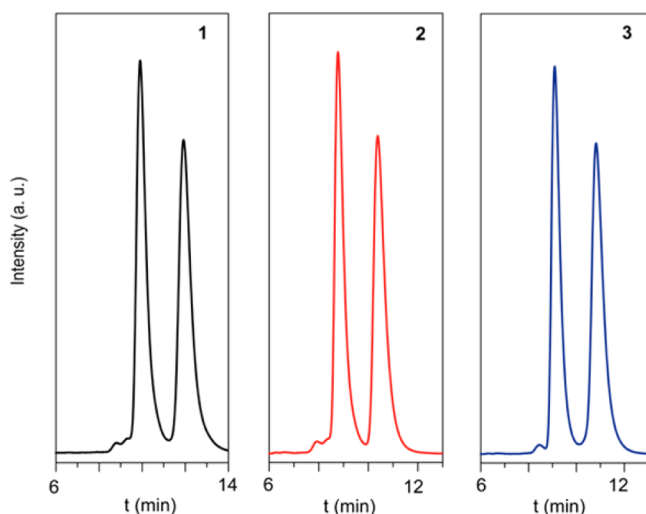


Figure 3. HPLC traces of racemic atropisomers of compounds 1–3 on a (*R,R*)-Whelk 01 chiral column (toluene/iPrOH 9/1 as eluent; flow rate 4 mL/min).

However, the formation of both stereoisomers in the synthesis of BNPCs 1–3 has been unambiguously demon-

strated by HPLC on a chiral stationary phase (column (*R,R*)-Whelk 01) and a binary toluene/iPrOH mixture (9/1) under isocratic conditions (Figure 3). The two enantiomers of 1 and the two diastereomers of 2 and 3 were separated under these conditions at room temperature. As stated before, in the reaction conditions, there is no preference for any of the possible stereoisomers of compounds 1–3 and, consequently, the amounts of both *M* and *P* stereoisomers are equal for all of the reported BNPCs. In fact, the circular dichroism spectra (CD) of the isolated compounds 1–3 show no dichroic response.

CD spectroscopy has been utilized to unambiguously demonstrate the successful separation of the stereoisomers of 1–3 in a good solvent such as CH_2Cl_2 . Thus, in all the studied BNPCs, the CD spectra of both peaks 1 and 2 are mirror images, the dichroic pattern always being the same for each separated peak regardless of the peripheral substitution (Figure 4). The CD spectra of both peaks of each stereoisomer show a beautiful double-bisignated Cotton effect with dichroic maxima at 237, 266, 296, and 306 nm and zero-crossing points at 250, 278, and 303 nm. These data can be reasonably assigned to electronic transitions at the aromatic units.

Unfortunately, all our attempts to obtain crystals suitable for the determination of the crystalline structure of all the stereoisomers investigated have been unfruitful and, therefore, we cannot assign unambiguously the absolute configuration of the atropisomers. Despite that, the CD spectra of the separated stereoisomers demonstrate that, under these experimental conditions, the axial chirality prevails over the point chirality.

The studied BNPCs have been designed to possess suitable functional groups—mainly large aromatic units and amides that induce π -stacking and the formation of H-bonding arrays, respectively—that favor an efficient self-assembly. The first insights into the self-assembly of compounds 1–3 can be obtained by FTIR and concentration-dependent ^1H NMR spectroscopy. Thus, the FTIR spectra of 1–3 show well-defined bands at around 3320, 1635, and 1545 cm^{-1} corresponding to bound N–H and amide I (C=O) stretching bands as well as the amide II (C–N) bending band.²¹ Furthermore, the participation of the side chains in the self-assembly of 1–3 is also inferred from the stretching bands of the paraffinic methylene groups that are observed at $\nu \sim 2925$, 2860, and 1465 cm^{-1} (Table S1 and Figure S1 in the Supporting Information).²² The formation of the H-bonding arrays between the amide functional groups is also inferred by the downfield shift experienced by the triplet at $\delta \sim 6.3$,

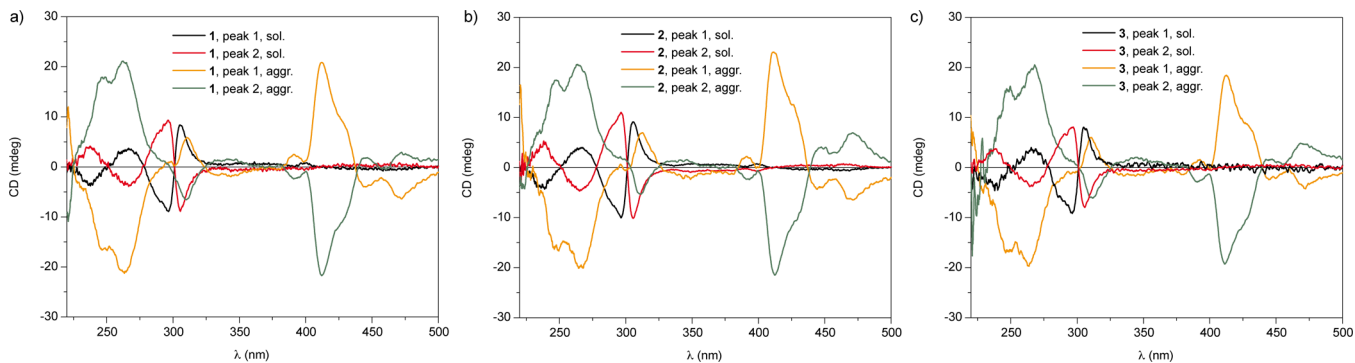


Figure 4. CD spectra of all stereoisomers of (a) 1, (b) 2, and (c) 3 in a molecularly dissolved state (sol., black and red lines; CH_2Cl_2 , 298 K, $\sim 1 \times 10^{-5}$ M) and in the aggregated state (aggr., green and orange lines; CH_2Cl_2 , 95/5, 298 K, $\sim 1 \times 10^{-5}$ M).

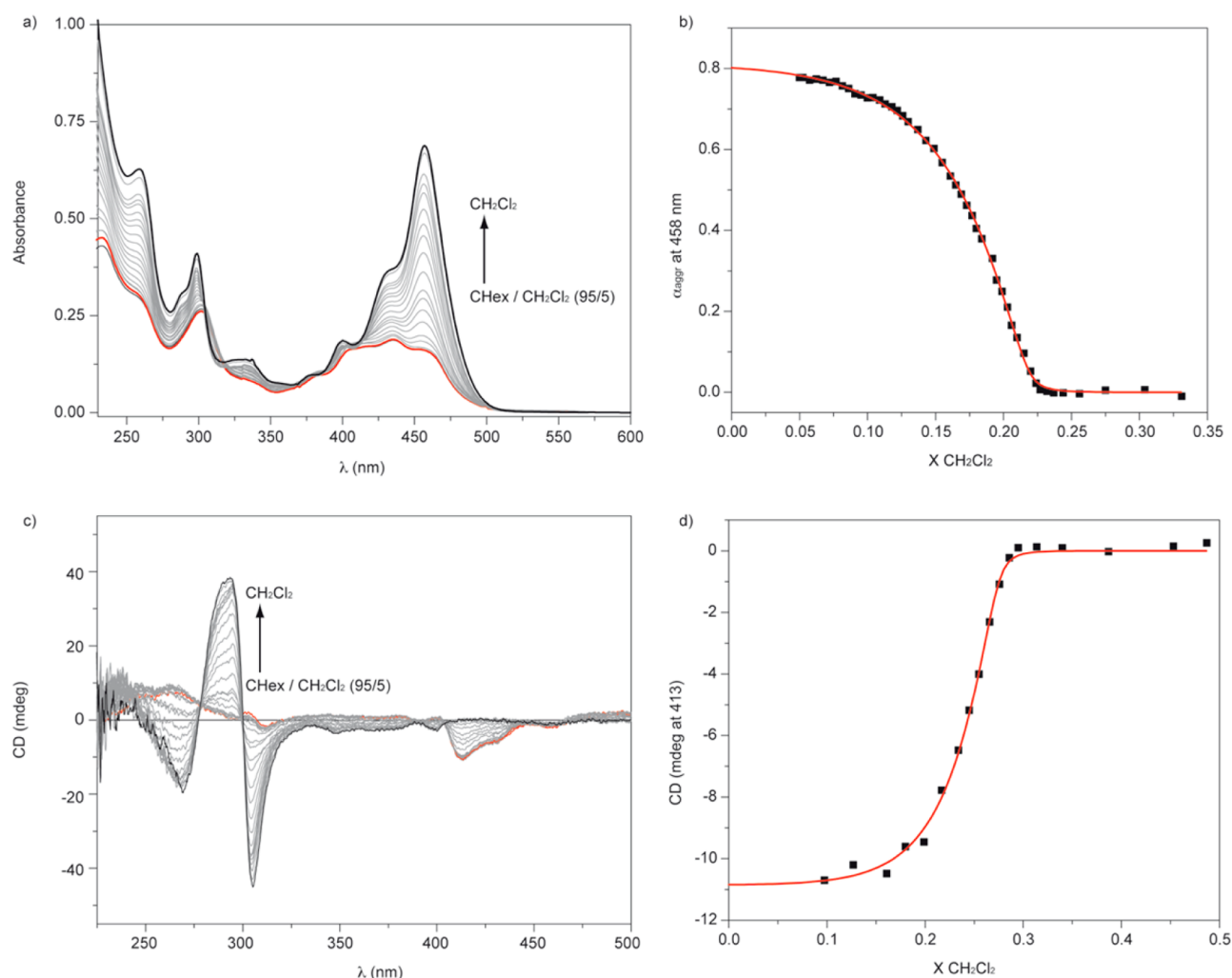


Figure 5. UV-vis spectra (a) and denaturation curve (b) of **1** in CHex/CH₂Cl₂ mixtures (1×10^{-5} M; 298 K) and CD spectra (c) and denaturation curve (d) of peak 2 of compound **2** in CHex/CH₂Cl₂ mixtures (1×10^{-5} M; 298 K). The red lines in (b) and (d) depict the fitting to the SD model.

corresponding to the amide, in concentration-dependent ¹H NMR experiments (Figure S2 in the Supporting Information).

We have recently reported that the supramolecular polymerization of a closely related NPDC is accompanied of drastic spectroscopic changes in the corresponding UV-vis spectra that make this technique suitable to follow the self-assembly of this class of chromophores.¹⁷ In good analogy with this molecule, the UV-vis spectra of the three studied BNPCs in a good solvent such as CH₂Cl₂ exhibit an intense band with vibronic fine structure, typical of molecularly dissolved perylene-based systems, centered at 454 nm and shoulders at 428 and 399 nm (Figure S3 in the Supporting Information).⁹ Unfortunately, compounds **1–3** are scarcely soluble in apolar solvents such as methylcyclohexane, heptane, and cyclohexane (CHex). However, it is possible to see a clear broadening effect in the UV-vis spectra of these compounds diagnostic of the efficient aggregation by using a 95/5 mixture of CHex/CH₂Cl₂ (Figure S3).⁹ By using these experimental conditions, we have investigated the effect exerted by the aggregation of the stereoisomers of **1–3** in the CD pattern. As in the case of the UV-vis spectra, the aggregation significantly changes the CD spectra of both peak 1 and peak 2 of the three BNPCs **1–3** (Figure 4). In the aggregated state, the intense peak at 306 nm is practically canceled and a remarkable red shift is observed

with a dichroic maximum at 413 nm. This 100 nm shift of the maximum is clearly ascribed to the supramolecular polymerization of the studied BNPCs and coincides with the lowest energy band observed in the UV-vis spectra. Interestingly, the six diastereomers of **1–3** exhibit a dichroic pattern which coincides with that observed in the molecularly dissolved state (Figure 4). The three peaks 1 show a \pm pattern in the most intense bands ascribable to a right-handed helicity and vice versa. These experimental data confirm, once again, the preponderance of atropisomerism over point chirality.

Mechanism of Supramolecular Polymerization. The function of supramolecular polymers is closely related to the mechanism followed by the monomeric units to self-assemble. From a mechanistic point of view, there are two basic mechanisms reported for the supramolecular polymerization of chiral organic molecules, isodesmic and cooperative. In the former, all of the chemical equilibria yielding the aggregate exhibit the same constant, while in the latter, there are two extreme regimens, nucleation and elongation, that finally yield the supramolecular polymer.⁷ The accurate investigation of the supramolecular polymerization mechanism is often carried out by using variable temperature (VT) spectroscopy, usually UV-vis or CD.^{7,12,17} In the case of atropisomers, these VT experiments could induce the racemization, thus decreasing the

Table 1. Thermodynamic Parameters Associated with the Cooperative Supramolecular Polymerization Mechanism of Compounds 1–3 at 298 K

compd	ΔG^c	m	$\Delta G'^c$	K_e	σ	K_n
1 ^a	-39.2(±2.2)	50.0(±1.2)	-36.7	2.71×10^6 ^d	1.8×10^{-3}	4.88×10^3
1, peak 1 ^b	-45.6(±1.3)	66.0(±5.7)	-42.3	2.60×10^7 ^e	6.8×10^{-3}	1.77×10^5
2 ^a	-40.7(±1.1)	50.0(±5.6)	-38.2	4.97×10^6 ^d	4.1×10^{-2}	2.04×10^5
2, peak 2 ^b	-42.7(±1.7)	61.9(±7.2)	-39.6	8.76×10^6 ^e	6.6×10^{-3}	5.78×10^4
3 ^a	-39.6(±4.7)	57.3(±2.8)	-36.7	2.75×10^6 ^d	2.3×10^{-2}	6.32×10^4
3, peak 2 ^b	-47.5(±1.1)	83.6(±5.7)	-43.3	3.92×10^7 ^e	2.1×10^{-2}	8.24×10^5

^aDerived by using UV–vis spectroscopy. ^bDerived by using CD spectroscopy. ^cCalculated at a molar fraction of the good solvent $f = 0.05$ that corresponds to the mixture CHex/CH₂Cl₂ 95/5. ^dThese elongation constants correspond to the formation of heterochiral aggregates ($K_{e,HET}$). ^eThese elongation constants correspond to the formation of homochiral aggregates ($K_{e,HOMO}$).

enantiopurity of the samples. To solve this drawback, we have utilized the solvent-denaturation (SD) model in which the self-assembly of a system is considered as a function of the ratio between a good and a poor solvent that favors the solvation of the monomer and the aggregation, respectively.¹⁸

We have first investigated the mechanism of the mixture of the stereoisomers of compounds 1–3. Since this mixture is CD-silent, solvent-dependent UV–vis experiments have been developed (Figure 5). We have already showed the spectroscopic changes experienced by 1–3 by using a good solvent such as CH₂Cl₂ and a 95/5 mixture of CHex/CH₂Cl₂ (Figure S3 in the Supporting Information). An increasing amount of CH₂Cl₂ results in an intense increase in the band centered at 458 nm (Figure 5a,b and Figure S4 in the Supporting Information). Plotting the variation of the degree of aggregation (α) at 458 nm against the solvent composition results in nonsigmoidal curves for the three BNPCs 1–3 characteristic of a cooperative mechanism.⁷ Fitting these nonsigmoidal curves with the SD model allows deriving the Gibbs free energy of monomer association (ΔG) and the parameter m that relates the ability of the good solvent to associate with the monomer, thereby destabilizing the supramolecular polymers. The derived thermodynamic parameters together with the degree of cooperativity σ are collected in Table 1. The calculated ΔG and σ values are in the range of some other self-assembling molecules such as benzene tricarboxamides and C₃-symmetric oligo(phenylene ethynylene) tricarboxamides.²³

It is worth noting that the aforementioned values correspond to the racemic mixture of the stereoisomers of the investigated compounds 1–3. An intriguing question is elucidating the influence of separating the corresponding stereoisomers on the supramolecular polymerization mechanism. Thus, considering the enormous differences found in the CD spectra of the stereoisomers of 1–3 by using a good solvent such as CH₂Cl₂ and a 95/5 mixture of CHex and CH₂Cl₂, we have performed denaturation experiments of peak 1 of compound 1 and peak 2 of compounds 2 and 3 by using CD spectroscopy. The changes in the CD spectra of these three enantiopure stereoisomers are depicted in Figure 5c,d and Figure S5 in the Supporting Information. Increasing the amount of the good solvent produces the apparition of the CD pattern (maxima at 237, 266, 296, and 306 nm) characteristic of the molecularly dissolved state and the depletion of the dichroic signal at 413 nm. Plotting the variation of the CD response at 413 nm against the amount of good solvent yields nonsigmoidal curves that can be fitted to the SD model. The derived thermodynamic parameters, in the range of -40 kJ mol^{-1} , are similar to those derived for the racemic mixture (Table 1). However, the m

parameter is higher for the enantiomerically enriched stereoisomers than for the racemic mixture. Equations 1–3 allow calculating the Gibbs free energy gain upon monomer addition ($\Delta G'$) depending on the molar fraction of good solvent (m) as well as the corresponding nucleation (K_n) and elongation (K_e) constants (Table 1).¹⁸

$$\Delta G' = \Delta G + mf \quad (1)$$

$$\Delta G' = -RT \ln K_e \quad (2)$$

$$\sigma = K_n/K_e \quad (3)$$

In the case of the racemic mixture of 1–3, these binding constants correspond to the formation of heterochiral aggregates ($K_{e,HET}$), while the enantiomerically enriched peaks of 1–3 relate to the formation of homochiral aggregates ($K_{e,HOMO}$). The derived values of the elongation binding constants $K_{e,HOMO}$ are higher than those calculated for $K_{e,HET}$, which implies that the formation of homochiral aggregates is favored.

Amplification of Chirality. A number of supramolecular polymers constituted by monomeric units decorated with side chains exhibiting point chirality have been reported to exhibit amplification of chirality.^{6,8,11,12,23} To control and investigate this phenomenon in covalent and supramolecular polymers, directly related with the origin of homochirality in nature, *sergeants-and-soldiers* (SaS) and *majority rules* (MR) experiments have been described. In the former, the chirality of a racemic mixture of two enantiomers (soldiers) is biased by the addition of increasing amounts of an enantiomerically enriched congener (sergeants). In the latter, a slight excess of one of the stereoisomers conditions the whole chirality of the mixture to that of this stereoisomer. In both cases, a nonlinear increment of the dichroic response is the fingerprint of biasing the chirality of the mixture. The synthesis and chiral separation of the stereoisomers of BNPCs 1–3 provides up to six different stereoisomers that allow developing a variety of SaS and MR experiments and contribute to shedding light on the amplification of chirality phenomena by using chiral units with asymmetry elements other than point chirality.

We first performed a SaS experiment in aggregated conditions (CHex/CH₂Cl₂, 95/5, $1 \times 10^{-5} \text{ M}$) by mixing the racemic mixture of the two enantiomers of 1 with peak 1 of compound 2 (Figure 6a and Figure S6a in the Supporting Information). The addition of increasing amounts of peak 1 of compound 2 to the racemic mixture of 1 results in the apparition of a dichroic response (Figure S6a). Plotting the variation of the dichroic signal at 413 nm against the enantiomeric excess of the mixture results in a straight line,

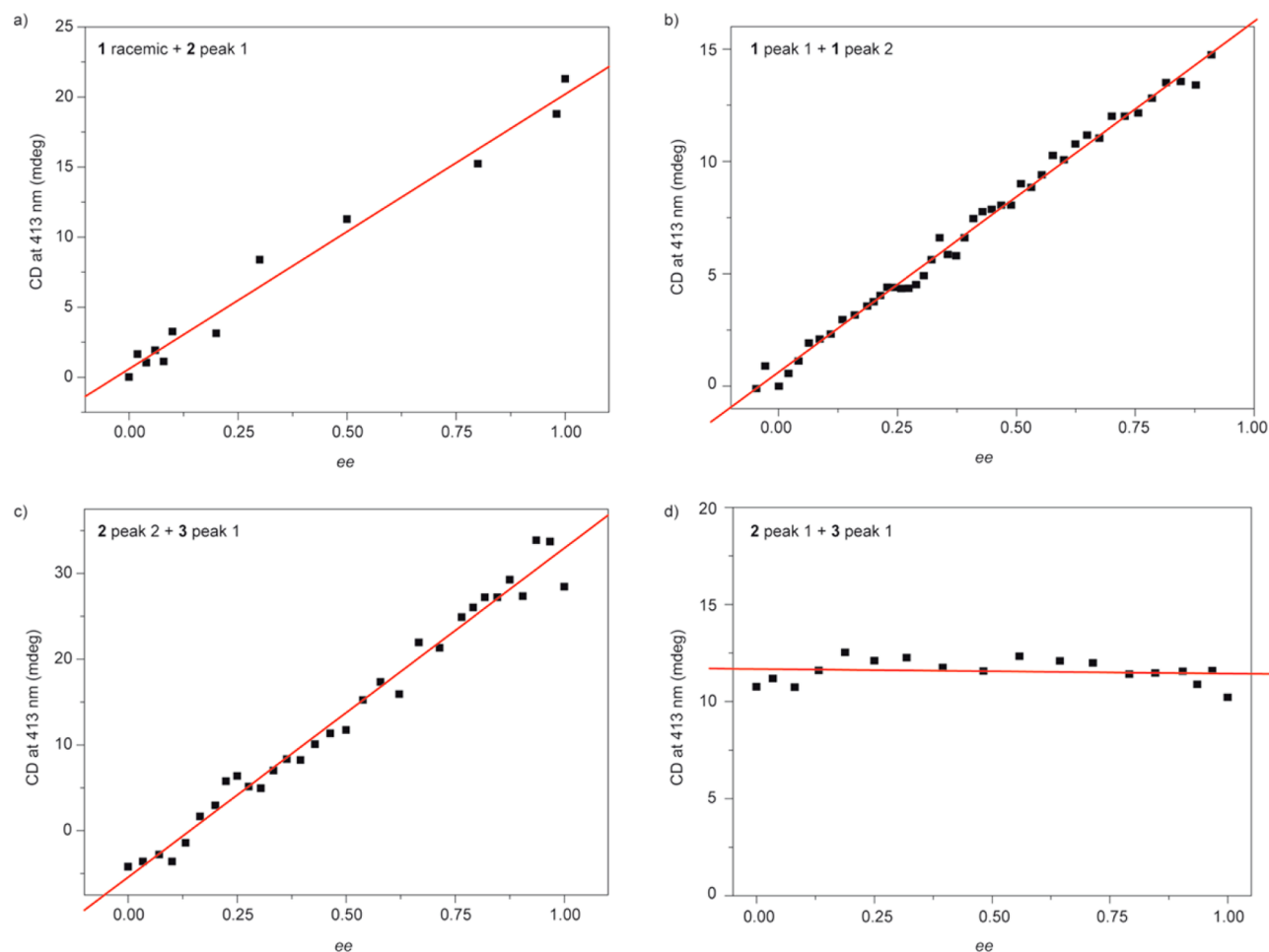


Figure 6. Changes in CD intensity as a function of ee in the SaS experiment performed with the racemic mixture of **1** and peak 2 of compound **1** (a), MR experiments performed with the two enantiomers of compound **1** (peaks 1 and 2) (b), two diastereomers of compounds **2** and **3** (peaks 2 and 1) (c), and the two diastereomers with the same axial chirality (peak 1) of compounds **2** and **3** (d). All experiments were performed in a 95/5 CHex/CH₂Cl₂ mixture at 298 K and at a concentration of $\sim 1 \times 10^{-5}$ M. The red lines in (a)–(d) depict the fitting to the variation of the CD intensity to a linear regression.

diagnostic of the lack of amplification of chirality in this mixture (Figure 6a).

To further investigate this phenomenon in atropisomers, we have carried out two different MR experiments. In the first of them, we have mixed different amounts of peaks 1 and 2 of compound **1**: that is, we have mixed together two enantiomers with no point but with axial chirality. The second of these MR experiments consists of mixing different amounts of peak 2 of compound **2** and peak 1 of compound **3**, keeping the total concentration constant. To the best of our knowledge, this MR experiment is the first in which two enantiomers with two different elements of chirality have been mixed up to investigate the amplification of chirality. In both MR experiments a dichroic response is observed at high enantiomeric excess (ee) (Figure S6b,c in the Supporting Information). However, unlike those examples of MR reported for molecules endowed with stereogenic centers at the side chains, the increasing dichroic response follows a linear trend in the mixture of the two peaks of compound **1** (Figure 6b,c). These results, also observed in the second MR experiment, indicate the supremacy of axial versus point chirality that does not allow any amplification of chirality. Finally, we have developed a nonclassical MR experiment in which two diastereomers are mixed. Thus, we have mixed different amounts of peak 1 of both **2** and **3** (Figure

S6d). In this experiment, the chirality of the mixed stereoisomers only differs in the point chirality but not in the axial chirality, the CD spectra of both being identical. In this case, neither an additive nor a diminishing effect in the CD response is observed (Figure 6d). In fact, a straight line with zero slope is obtained upon plotting the CD response at 413 nm versus the ee of peak 1 of **3**.

The variety of amplification of chirality experiments performed by using different mixtures of stereoisomers showing atropisomerism or atropisomerism and point chirality clearly demonstrates that axial chirality predominates over point chirality. Interestingly, the chiral character of all compounds utilized in these amplification of chirality studies can be considered as a relevant example of self-sorting in which a competence between the formation of homochiral or heterochiral aggregates can operate.²⁴ The calculated thermodynamic data reveal that $K_{e,HOMO}$ values are higher than $K_{e,HET}$ values (see data in Table 1) and, consequently, self-recognition (narcissistic self-sorting) prevails over self-discrimination (social self-sorting) that yields preferentially homochiral aggregates. If a self-recognition effect is operating in the amplification of chirality experiments, an equal amount of *M* or *P* aggregated atropisomers is formed upon the addition of the corresponding stereoisomer together with the excess of the

added atropisomer. The net result of having an equal amount of homoaggregates is a CD-silent mixture. Under these conditions only the excess of the added atropisomer is detected, thus resulting in a straight line.

CONCLUSIONS

We describe herein the synthesis of three BNPCs peripherally decorated with achiral (**1**) or chiral (**2** and **3**) side chains. The restricted rotation of the two *N*-annulated perylene moieties results in the formation of atropisomers (enantiomers and diastereomers) that can be separated by chiral HPLC. Circular dichroism has been utilized to investigate the chiroptical features of the six stereoisomers obtained from **1**–**3**. The corresponding CD spectra show a beautiful pattern in a good solvent (CH₂Cl₂) that changes drastically upon adding a poor solvent (CHex) which favors the aggregation. The denaturation experiments performed with these atropisomers reveal a cooperative mechanism in which the formation of homochiral aggregates (narcissistic self-sorting) is favored over the formation of heterochiral (social self-sorting) aggregates. These thermodynamic data support the experimental evidence attained by the amplification of chirality experiments that demonstrate the supremacy of axial chirality over point chirality. The results presented herein shed relevant light on the structural conditions exhibited by molecular units endowed with different elements of asymmetry to generate chiral supramolecular structures and the predominance of some elements of asymmetry (axial chirality) over other (point chirality) in the origin of homochirality.

EXPERIMENTAL SECTION

General Methods. All solvents were dried according to standard procedures. Reagents were used as purchased. All air-sensitive reactions were carried out under an argon atmosphere. Flash chromatography was performed using silica gel. Analytical thin-layer chromatography (TLC) was performed using aluminum-coated plates. NMR spectra were recorded on a 300 MHz (¹H, 300 MHz; ¹³C, 75 MHz) spectrometer using partially deuterated solvents as internal standards. Coupling constants (*J*) are denoted in Hz and chemical shifts (δ) in ppm. Multiplicities are denoted as follows: s = singlet, d = doublet, t = triplet, m = multiplet, br = broad. UV–vis spectra were registered by using 1 cm path length quartz cuvettes. Circular dichroism (CD) measurements were performed in the continuous mode between 500 and 220 nm, with a wavelength increment of 1 nm, a response time of 1 s, and a bandwidth of 2 nm with 1 cm path length quartz cuvettes. Spectra from three scans were averaged. HPLC experiments were conducted using a (*R,R*)-Whelk 01 (5/100) chiral column (25 cm \times 10 mm) with a toluene/2-propanol mixture (9/1) as eluent.

Compounds **4**–**6**, **8a**–**c**, and **9a** were prepared according to previously reported synthetic procedures and showed spectroscopic properties identical with those reported therein.^{17,19,25}

3-Bromo-1-decyl-1*H*-phenanthro[1,10,9,8-*cdefg*]carbazole (7**).** Compound **6** (0.19 g, 0.48 mmol), was dissolved in DMF (8 mL). The mixture was cooled to 0 °C, and then *N*-bromosuccinimide (NBS) (0.09 g, 0.48 mmol) was added. The reaction mixture was stirred at 0 °C for 30 min. The residue was washed with water and brine, extracted with chloroform, and dried over MgSO₄. After evaporation of the solvent, the residue was purified by column chromatography (silica gel, hexane), affording compound **7** as a yellow solid (0.14 g, 60%): ¹H NMR (CDCl₃, 300 MHz) δ 8.68 (1H, H₄ or ₅, d, *J* = 5.2 Hz), 8.65 (1H, H₅ or ₄, d, *J* = 5.2 Hz), 8.34 (1H, H₉, d, *J* = 8.1 Hz), 8.14 (1H, H₂, d, *J* = 8.1 Hz), 8.12 (1H, H₁, s), 8.00–7.74 (4H, H₃ or ₆ or ₆ or ₃ or ₇ or ₈, br), 4.64 (2H, H₁₀, t, *J* = 6.9 Hz), 2.08 (2H, H_b, m), 1.40–1.17 (14H, H_{c+d+e+f+g+h+i+j}, br), 0.85 (3H, H_p, t, *J* = 6.7 Hz); ¹³C NMR (CDCl₃, 75 MHz) δ 132.1, 131.4, 130.5, 129.8, 128.7, 127.9,

125.4, 125.3, 124.8, 124.8, 124.6, 124.4, 121.5, 121.2, 117.6, 117.2, 113.4, 46.0, 32.0, 31.3, 29.9, 29.6, 29.5, 29.4, 27.2, 22.8, 14.2; FTIR (neat) 728, 802, 1260, 1309, 1376, 1471, 1561, 2853, 2925, 2954, 3050 cm⁻¹; HRMS (MALDI-TOF, exact mass) calcd for C₃₀H₃₁BrN [M + H]⁺ 484.1639, found 484.1661; mp 116–117 °C.

(S)-(4-(3,7-Dimethyloctyl)carbamoyl)phenyl)boronic Acid (9b**).** 4-(Dihydroxyboryl)benzoic acid (0.75 g, 4.50 mmol), 1-ethyl-3-(3-dimethylamino-propyl)carbodiimide hydrochloride (0.95 g, 5.00 mmol), and 4-dimethylaminopyridine (0.61 g, 5.00 mmol) were dissolved in dry methylene chloride (37 mL) and dry DMSO (1 mL) under an argon atmosphere. The mixture was cooled to 0 °C and stirred for 15 min. Then, compound **8b** (0.78 g, 5.00 mmol) was added portionwise. The reaction mixture was stirred at room temperature for 42 h. The organic layer was washed with water and 1 M HCl, and the precipitate was filtered, affording compound **9b** as a white solid (0.80 g, 58%): ¹H NMR (CD₃OD, 300 MHz) δ 7.75 (4H, H₁₊₂, br), 3.41 (2H, H_a, m), 1.67–1.16 (10H, H_{b+c+e+f+g+i+j}, m), 0.95 (3H, H_d, d, *J* = 6.4 Hz), 0.87 (6H, H_p, d, *J* = 6.6 Hz); ¹³C NMR (CD₃OD, 75 MHz) δ 170.2, 134.8, 127.2, 40.4, 39.1, 38.3, 37.5, 31.9, 29.1, 25.8, 23.0, 20.0; FTIR (neat) 627, 653, 710, 852, 941, 1013, 1116, 1272, 1368, 1459, 1515, 1555, 1623, 2464, 2551, 2871, 2925, 2957, 3303, 3440 cm⁻¹; HRMS (MALDI-TOF, exact mass) calcd for C₁₇H₂₈BNO₃ [M]⁺, 305.2162, found 305.2197; mp 210–211 °C.

(R)-(4-(3,7-Dimethyloctyl)carbamoyl)phenyl)boronic Acid (9c**).** 4-(Dihydroxyboryl)benzoic acid (0.61 g, 3.65 mmol), 1-ethyl-3-(3-(dimethylamino)propyl)carbodiimide hydrochloride (0.77 g, 4.01 mmol), and 4-dimethylaminopyridine (0.49 g, 4.01 mmol) were dissolved in dry methylene chloride (30 mL) and dry DMSO (0.8 mL) under an argon atmosphere. The mixture was cooled to 0 °C and stirred for 20 min. Then, compound **8c** (0.63 g, 4.01 mmol) was added portionwise. The reaction mixture was stirred at room temperature for 40 h. The organic layer was washed with water and 1 M HCl, and the precipitate was filtered, affording compound **9c** as a white solid (0.67 g, 60%): ¹H NMR (CD₃OD, 300 MHz) δ 7.78 (4H, H₁₊₂, m), 3.42 (2H, H_a, m), 1.73–1.06 (10H, H_{b+c+e+f+g+i+j}, m), 0.94 (3H, H_d, d, *J* = 6.4 Hz), 0.86 (6H, H_p, d, *J* = 6.6 Hz); ¹³C NMR (CD₃OD, 75 MHz) δ 170.2, 137.1, 134.9, 134.8, 127.1, 40.4, 39.1, 38.3, 37.5, 31.9, 29.1, 25.7, 23.1, 23.0, 20. ; FTIR (neat) 643, 715, 803, 850, 1006, 1023, 1116, 1149, 1193, 1272, 1350, 1396, 1507, 1537, 1612, 1629, 2869, 2922, 2954, 3312 cm⁻¹; HRMS (MALDI-TOF, exact mass) calcd for C₁₇H₂₈BNO₃ [M]⁺ 305.2162, found 305.2149; mp 210–211 °C.

***N*-Decyl-4-(1-decyl-1*H*-phenanthro[1,10,9,8-*cdefg*]carbazol-3-yl)benzamide (**10a**).** Compound **7** (0.37 g, 0.76 mmol), compound **9a** (0.93 g, 3.04 mmol), and tetrakis(triphenylphosphine)-palladium(0) (0.09 g, 0.08 mmol) were dissolved in THF (150 mL). K₂CO₃ (0.53 g, 3.80 mmol) was dissolved in water (8 mL) and added to the solution under an argon atmosphere. The reaction mixture was heated at reflux for 40 h. After evaporation of the solvent under reduced pressure, the residue was washed with water, extracted with chloroform, and dried over MgSO₄. After evaporation of the solvent, the residue was purified by column chromatography (silica gel, chloroform), affording compound **10a** as a yellow solid (0.25 g, 49%): ¹H NMR (CDCl₃, 300 MHz) δ 8.61 (2H, H₄₊₅, d, *J* = 7.6 Hz), 8.11 (1H, H₂ or ₇, d, *J* = 8.0 Hz), 8.05 (1H, H₇ or ₂, d, *J* = 8.1 Hz), 7.95 (2H, H₁₁, d, *J* = 8.2 Hz), 7.90–7.64 (7H, H₁₊₃₊₆₊₈₊₉₊₁₀, m), 6.39 (1H, H_w, t, *J* = 5.5 Hz), 4.53 (2H, H_p, t, *J* = 6.8 Hz), 3.53 (2H, H_b, m), 2.00 (2H, H_m, m), 1.68 (2H, H_n, m), 1.50–1.07 (28H, H_{d+e+f+g+h+i+j+n+o+p+q+r+s+u}, br), 0.91 (3H, H_v, t, *J* = 7.1 Hz), 0.85 (3H, H_q, t, *J* = 7.1 Hz); ¹³C NMR (CDCl₃, 75 MHz) δ 167.5, 145.3, 136.1, 133.5, 132.1, 131.6, 130.7, 130.5, 130.3, 128.7, 127.5, 127.2, 125.1, 125.0, 124.7, 124.7, 124.0, 123.8, 121.0, 120.9, 117.3, 117.2, 114.2, 113.3, 45.8, 40.4, 32.0, 31.9, 31.3, 29.9, 29.7, 29.7, 29.6, 29.6, 29.5, 29.4, 29.3, 27.2, 22.8, 22.7, 14.3, 14.2; FTIR (neat) 759, 808, 852, 987, 1308, 1371, 1471, 1502, 1547, 1634, 2853, 2925, 3049, 3310 cm⁻¹; HRMS (MALDI-TOF, exact mass) calcd for C₄₇H₅₇N₂O [M + H]⁺ 665.4470, found 665.4488; mp 140–141 °C.

(S)-4-(1-Decyl-1*H*-phenanthro[1,10,9,8-*cdefg*]carbazol-3-yl)-*N*-(3,7-dimethyloctyl)benzamide (10b**).** Compound **7** (0.15 g, 0.30 mmol), compound **9b** (0.38 g, 1.20 mmol), tetrakis(triphenylphosphine)palladium(0) (0.04 mg, 0.03 mmol), and

K_2CO_3 (0.21 g, 1.60 mmol) were dissolved in THF (61.2 mL) and water (3.3 mL) under an argon atmosphere. The reaction mixture was heated at reflux for 24 h. After evaporation of the solvent under reduced pressure, the residue was washed with water, extracted with chloroform, and dried over $MgSO_4$. After evaporation of the solvent, the residue was purified by column chromatography (silica gel, chloroform), affording compound **10b** as a yellow solid (0.15 g, 73%): 1H NMR ($CDCl_3$, 300 MHz) δ 8.59 (2H, H_{4+5} , d, J = 7.6 Hz), 8.09 (1H, $H_{2\text{ or }7}$, d, J = 8.0 Hz), 8.04 (1H, $H_{7\text{ or }2}$, d, J = 8.3 Hz), 7.96 (2H, H_{11} , d, J = 8.2 Hz), 7.87–7.66 (7H, $H_{1+3+6+8+9+10}$, m), 6.36 (1H, H_a , t, J = 5.5 Hz), 4.50 (2H, H_b , t, J = 6.9 Hz), 3.58 (2H, H_b , m), 1.98 (2H, H_b , br), 1.76–1.18 (24H, $H_{c+d+f+g+h+i+j+m+n+o+p+q+r+s}$, br), 1.01 (3H, H_c , d, J = 6.4 Hz), 0.91 (6H, H_c , d, J = 6.6 Hz), 0.86 (3H, H_c , t, J = 7.0 Hz); ^{13}C NMR ($CDCl_3$, 75 MHz) δ 167.8, 145.6, 136.5, 133.8, 132.4, 131.9, 131.0, 130.9, 130.6, 129.0, 127.8, 127.5, 125.4, 125.3, 125.0, 124.9, 124.2, 124.1, 121.3, 121.2, 117.6, 117.5, 114.5, 113.6, 46.0, 39.7, 38.8, 37.7, 37.3, 32.4, 32.3, 31.6, 31.3, 30.2, 29.9, 29.9, 29.7, 28.4, 27.5, 25.2, 23.2, 23.1, 20.0, 14.5; FTIR (neat) 760, 808, 851, 988, 1140, 1196, 1308, 1374, 1470, 1503, 1547, 1634, 2855, 2925, 2954, 3049, 3306 cm^{-1} ; HRMS (MALDI-TOF, exact mass) calcd for $C_{47}H_{57}N_2O$ [$M + H$] $^+$ 665.4470, found 665.4491; mp 137–138 °C.

(R)-4-(1-Decyl-1H-biphenanthro[1,10,9,8-cdefg]carbazol-3-yl)-N-(3,7-dimethyloctyl)benzamide (10c). Compound **7** (0.16 g, 0.33 mmol), compound **9c** (0.20 g, 0.66 mmol), and tetrakis(triphenylphosphine)palladium(0) (0.04 g, 0.03 mmol) were dissolved in THF (65 mL). K_2CO_3 (0.23 g, 1.65 mmol) was dissolved in water (3.5 mL) and added to the solution under an argon atmosphere. The reaction mixture was heated at reflux for 22 h. After evaporation of the solvent under reduced pressure, the residue was washed with water, extracted with chloroform, and dried over $MgSO_4$. After evaporation of the solvent, the residue was purified by column chromatography (silica gel, chloroform), affording compound **10c** as a yellow solid (0.18 g, 80%): 1H NMR ($CDCl_3$, 300 MHz) δ 8.68 (1H, $H_{4\text{ or }5}$, d, J = 1.7 Hz), 8.65 (1H, $H_{5\text{ or }4}$, d, J = 1.7 Hz), 8.14 (1H, $H_{2\text{ or }7}$, d, J = 8.1 Hz), 8.08 (1H, $H_{7\text{ or }2}$, d, J = 8.2 Hz), 7.97 (2H, H_{11} , d, J = 8.4 Hz), 7.95–7.72 (7H, $H_{1+3+6+8+9+10+11}$, m), 6.25 (1H, H_a , t, J = 5.4 Hz), 4.65 (2H, H_b , t, J = 6.9 Hz), 3.58 (2H, H_b , m), 2.07 (2H, H_b , m), 1.81–1.13 (24H, $H_{c+d+f+g+h+i+j+m+n+o+p+q+r+s}$, br), 1.01 (3H, H_c , d, J = 6.3 Hz), 0.91 (6H, H_c , d, J = 6.3 Hz), 0.85 (3H, H_c , t, J = 6.9 Hz); ^{13}C NMR ($CDCl_3$, 75 MHz) δ 167.5, 145.4, 136.3, 133.5, 132.3, 131.7, 131.7, 130.6, 130.4, 128.8, 127.6, 127.1, 125.1, 124.8, 124.7, 124.0, 123.9, 121.1, 121.0, 117.4, 117.3, 114.3, 113.4, 45.9, 39.4, 38.5, 37.3, 37.0, 31.9, 31.3, 31.0, 29.6, 29.4, 28.1, 27.3, 24.9, 22.9, 22.8, 19.7, 14.2; FTIR (neat) 758, 801, 852, 1309, 1472, 1503, 1548, 1636, 2853, 2926, 3050, 3310 cm^{-1} ; HRMS (MALDI-TOF, exact mass) calcd for $C_{47}H_{57}N_2O$ [$M + H$] $^+$ 665.4470, found 665.4459; mp 137–138 °C.

4,4'-(1,1'-Didecyl-1H,1'H-[3,3'-biphenanthro[1,10,9,8-cdefg]carbazole]-10,10'-diyl)bis(N-decylbenzamide) (1). A mixture of compound **10a** (0.66 g, 0.10 mmol), $Sc(OTf)_3$ (0.05 g, 0.10 mmol), and DDQ (0.02 g, 0.01 mmol) in toluene (15 mL) was stirred at room temperature for 22 h under an argon atmosphere. After evaporation of the solvent under reduced pressure, the product was washed with brine, extracted with chloroform, and dried over $MgSO_4$. The residue was then purified by column chromatography (silica gel, chloroform/methanol 10/0.05) to yield compound **1** as a yellow solid (0.04 g, 38%): 1H NMR ($CDCl_3$, 300 MHz) δ 8.70 (4H, $H_{4\text{ or }5}$, m), 8.15 (2H, $H_{5\text{ or }4}$, d, J = 8.3 Hz), 8.07 (2H, $H_{1\text{ or }8}$, s), 8.02 (4H, H_{10} , d, J = 8.2 Hz), 7.88–7.78 (10H, $H_{9+1\text{ or }8+2\text{ or }7+3\text{ or }6}$, m), 7.65 (2H, $H_{3\text{ or }6}$, t, J = 8.0 Hz), 6.40 (2H, H_a , t, J = 5.8 Hz), 4.65 (4H, H_b , t, J = 6.8 Hz), 3.57 (4H, H_b , m), 2.10 (4H, H_m , m), 1.72 (4H, H_c , m) 1.53–1.10 (56H, $H_{d+e+f+g+h+i+j+n+o+p+q+r+s+t}$, br), 0.92 (6H, H_c , t, J = 7.1 Hz), 0.80 (6H, H_c , t, J = 7.1 Hz); ^{13}C NMR (d_8 -THF, 75 MHz) δ 166.5, 145.3, 137.5, 135.4, 135.0, 133.0, 132.7, 131.6, 131.3, 130.7, 130.2, 128.4, 127.9, 125.7, 125.5, 125.3, 125.2, 124.5, 121.7, 121.6, 117.9, 116.4, 115.4, 46.2, 40.4, 32.7, 32.6, 32.1, 30.8, 30.5, 30.4, 30.3, 30.2, 30.1, 30.0, 30.0, 27.9, 23.4, 23.3, 14.3, 14.2; FTIR (neat) 513, 760, 802, 853, 1021, 1101, 1305, 1460, 1503, 1543, 1635, 2854, 2924, 3041, 3307 cm^{-1} ; HRMS (MALDI-TOF, exact mass) calcd for $C_{94}H_{111}N_4O_2$ [$M + H$] $^+$ 1327.8707, found 1327.8767; mp >270 °C.

4,4'-(1,1'-Didecyl-1H,1'H-[3,3'-biphenanthro[1,10,9,8-cdefg]carbazole]-10,10'-diyl)bis(N-((S)-3,7-dimethyloctyl)-benzamide) (2). A mixture of compound **10b** (0.13 g, 0.20 mmol), $Sc(OTf)_3$ (0.1 g, 0.20 mmol), and DDQ (0.05 mg, 0.20 mmol) in toluene (30 mL) was stirred at room temperature for 22 h under an argon atmosphere. The solvent was evaporated under reduced pressure, and the product was washed with brine, extracted with chloroform, and dried over $MgSO_4$. After evaporation of the solvent, the residue was purified by column chromatography (silica gel, hexane/chloroform 1/1) to yield the yellow solid product **2** (0.12 g, 45%): 1H NMR ($CDCl_3$, 300 MHz) δ 8.76 (2H, $H_{4\text{ or }5}$, d, J = 7.8 Hz), 8.10 (2H, $H_{5\text{ or }4}$, d, J = 7.6 Hz), 8.15 (2H, $H_{2\text{ or }7}$, d, J = 8.3 Hz), 8.10 (2H, $H_{1\text{ or }8}$, s), 8.00 (4H, H_{10} , d, J = 8.2 Hz), 7.87–7.81 (10H, $H_{9+1\text{ or }8+2\text{ or }7+3\text{ or }6}$, m), 7.65 (2H, $H_{6\text{ or }3}$, t, J = 7.8 Hz), 6.22 (2H, H_a , t, J = 5.4 Hz), 4.76 (4H, H_b , t, J = 6.8 Hz), 3.59 (4H, H_b , m), 2.15 (4H, H_b , q, J = 7.4 Hz), 1.75–1.16 (48H, $H_{c+d+f+g+h+i+j+m+n+o+p+q+r+s}$, br), 1.01 (6H, H_c , d, J = 6.4 Hz), 0.90 (12H, H_c , d, J = 6.6 Hz), 0.79 (6H, H_c , t, J = 7.0 Hz); ^{13}C NMR (d_8 -THF, 75 MHz) δ 166.2, 145.0, 137.1, 134.7, 132.6, 132.4, 132.1, 131.2, 131.0, 130.3, 129.9, 128.1, 127.5, 125.4, 125.2, 124.9, 124.7, 124.1, 121.3, 121.2, 117.6, 117.4, 115.9, 114.7, 45.8, 39.7, 38.1, 37.7, 37.5, 32.1, 31.6, 31.2, 29.9, 29.8, 29.6, 29.5, 28.4, 27.5, 22.8, 22.5, 22.4, 19.5, 13.7; FTIR (neat) 758, 804, 852, 1301, 1339, 1466, 1505, 1542, 1635, 2855, 2925, 2954, 3048, 3322 cm^{-1} ; HRMS (MALDI-TOF, exact mass) calcd for $C_{94}H_{111}N_4O_2$ [$M + H$] $^+$ 1327.8707, found 1327.8735; mp >270 °C.

4,4'-(1,1'-Didecyl-1H,1'H-[3,3'-biphenanthro[1,10,9,8-cdefg]carbazole]-10,10'-diyl)bis(N-((R)-3,7-dimethyloctyl)-benzamide) (3). A mixture of compound **10c** (0.18 g, 0.27 mmol), $Sc(OTf)_3$ (0.13 g, 0.27 mmol), and DDQ (0.06 g, 0.27 mmol) in toluene (40 mL) was stirred at room temperature for 48 h under an argon atmosphere. After evaporation of the solvent under reduced pressure, the product was washed with brine, extracted with chloroform, and dried over $MgSO_4$. The residue was then purified by column chromatography (silica gel, chloroform) to yield compound **3** as a yellow solid (0.15 g, 42%): 1H NMR ($CDCl_3$, 300 MHz) δ 8.74 (4H, $H_{4\text{ or }5}$, m), 8.15 (2H, $H_{2\text{ or }7}$, d, J = 8.2 Hz), 8.09 (2H, $H_{1\text{ or }8}$, s), 8.00 (4H, H_{10} , d, J = 8.2 Hz), 7.90–7.78 (10H, $H_{9+1\text{ or }8+2\text{ or }7+3\text{ or }6}$, m), 7.67 (2H, $H_{3\text{ or }6}$, t, J = 7.9 Hz), 6.23 (2H, H_a , t, J = 5.4 Hz), 4.76 (4H, H_b , t, J = 6.6 Hz), 3.59 (4H, H_b , m), 2.14 (4H, H_b , m), 1.80–1.08 (48H, $H_{c+d+f+g+h+i+j+m+n+o+p+q+r+s}$, br), 1.01 (6H, H_c , d, J = 6.4 Hz), 0.90 (12H, H_c , d, J = 6.6 Hz), 0.79 (6H, H_c , t, J = 7.0 Hz); ^{13}C NMR (d_8 -THF, 75 MHz) δ 164.4, 143.1, 135.4, 135.3, 132.9, 130.8, 130.6, 129.4, 129.2, 128.4, 128.0, 126.3, 125.7, 123.5, 123.3, 123.0, 122.9, 122.3, 119.4, 119.3, 115.8, 115.6, 112.8, 44.0, 37.9, 36.3, 35.8, 35.7, 30.2, 29.7, 29.4, 28.0, 27.9, 27.7, 27.6, 26.5, 25.6, 21.0, 20.6, 20.5, 17.6, 11.8; FTIR (neat) 759, 804, 854, 1305, 1467, 1502, 1544, 1636, 2855, 2924, 3049, 3314 cm^{-1} ; HRMS (MALDI-TOF, exact mass) calcd for $C_{94}H_{111}N_4O_2$ [$M + H$] $^+$ 1327.8707, found 1327.8629; mp >270 °C.

■ ASSOCIATED CONTENT

Supporting Information

The Supporting Information is available free of charge on the ACS Publications website at DOI: 10.1021/acs.joc.5b02309.

Figures S1–S6 and chemical compound information (PDF)

■ AUTHOR INFORMATION

Corresponding Author

*E-mail for L.S.: lusamar@quim.ucm.es.

Author Contributions

†These authors contributed equally.

Notes

The authors declare no competing financial interest.

■ ACKNOWLEDGMENTS

This work was supported by the MINECO of Spain (CTQ2014-53046-P), Comunidad de Madrid (NanoBIOSOMA, S2013/MIT-2807), and UCM (UCM-SCH-PR34/07-15826). J.B. and E.E.G. thank the MECED and Comunidad de Madrid, respectively, for their predoctoral grants.

■ REFERENCES

- (1) Gal, J. *Top. Curr. Chem.* **2013**, *340*, 1–20.
- (2) Qin, T.; Skrabala-Joiner, S.-L.; Khalil, Z. G.; Johnson, R. P.; Capon, R. J.; Porco, J. A., Jr *Nat. Chem.* **2015**, *7*, 234–240.
- (3) Vera, F.; Barberá, J.; Romero, P.; Serrano, J. L.; Ros, M. B.; Sierra, T. *Angew. Chem., Int. Ed.* **2010**, *49*, 4910–4914.
- (4) Iavicoli, P.; Xu, H.; Feldborg, L. N.; Linares, M.; Paradinas, M.; Stafström, S.; Ocal, C.; Nieto-Ortega, B.; Casado, J.; López Navarrete, J. T.; Lazzaroni, R.; De Feyter, S.; Amabilino, D. B. *J. Am. Chem. Soc.* **2010**, *132*, 9350–9362.
- (5) Labuta, J.; Hill, J. P.; Ishihara, S.; Hanyková, L.; Ariga, K. *Acc. Chem. Res.* **2015**, *48*, 521–529.
- (6) (a) Green, M. M.; Reidy, M. P.; Johnson, R. D.; Darling, G.; O'Leary, D. J.; Willson, G. *J. Am. Chem. Soc.* **1989**, *111*, 6452–6454. (b) Palmans, A. R. A.; Meijer, E. W. *Angew. Chem., Int. Ed.* **2007**, *46*, 8948–8968. (c) Babu, S. S.; Praveen, V. K.; Ajayaghosh, A. *Chem. Rev.* **2014**, *114*, 1973–2129.
- (7) (a) De Greef, T. F. A.; Smulders, M. M. J.; Wolffs, M.; Schenning, A. P. H. J.; Sijbesma, R. P.; Meijer, E. W. *Chem. Rev.* **2009**, *109*, 5687–5754. (b) Chen, Z.; Lohr, A.; Saha-Möller, C. R.; Würthner, F. *Chem. Soc. Rev.* **2009**, *38*, 564–584.
- (8) García, F.; Sánchez, L. *J. Am. Chem. Soc.* **2012**, *134*, 734–742.
- (9) Smulders, M. M. J.; Schenning, A. P. H. J.; Meijer, E. W. *J. Am. Chem. Soc.* **2008**, *130*, 606–611.
- (10) Ogi, S.; Stepanenko, V.; Sugiyasu, K.; Takeuchi, M.; Würthner, F. *J. Am. Chem. Soc.* **2015**, *137*, 3300–3307.
- (11) Hill, J. P.; Jin, W.; Kosaka, A.; Fukushima, T.; Ichihara, H.; Shimomura, T.; Ito, K.; Hashizume, T.; Ishii, N.; Aida, T. *Science* **2004**, *304*, 1481–1483.
- (12) Ajayaghosh, A.; Varghese, R.; George, S. J.; Vijayakumar, C. *Angew. Chem., Int. Ed.* **2006**, *45*, 1141–1144.
- (13) (a) Xie, Z.; Stepanenko, V.; Radacki, K.; Würthner, F. *Chem. - Eur. J.* **2012**, *18*, 7060–7070. (b) Kamada, T.; Aratani, N.; Ikeda, T.; Shibata, N.; Higuchi, Y.; Wakamiya, A.; Yamaguchi, S.; Kim, K. S.; Yoon, Z. S.; Kim, D.; Osuka, A. *J. Am. Chem. Soc.* **2006**, *128*, 7670–7678. (c) van Delden, R. A.; Mecca, T.; Rosini, C.; Feringa, B. L. *Chem. - Eur. J.* **2004**, *10*, 61–70. (d) Nuckolls, C.; Katz, T. J.; Castellanos, L. *J. Am. Chem. Soc.* **1996**, *118*, 3767–3768.
- (14) (a) Helmich, F.; Smulders, M. M. J.; Lee, C. C.; Schenning, A. P. H. J.; Meijer, E. W. *J. Am. Chem. Soc.* **2011**, *133*, 12238–12246. (b) Kumar, J.; Tsumatori, H.; Yuasa, J.; Kawai, T.; Nakashima, T. *Angew. Chem., Int. Ed.* **2015**, *54*, 5943–5947. (c) Aparicio, F.; Nieto-Ortega, B.; Nájera, F.; Ramírez, F. J.; López Navarrete, J. T.; Casado, J.; Sánchez, L. *Angew. Chem., Int. Ed.* **2014**, *53*, 1373–1377.
- (15) Zeng, Z.; Ishida, M.; Zafra, J. L.; Zhu, X.; Sung, Y. M.; Bao, N.; Webster, R. D.; Lee, B. S.; Li, R.-W.; Zeng, W.; Li, Y.; Chi, C.; López Navarrete, J. T.; Ding, J.; Casado, J.; Kim, D.; Wu, J. *J. Am. Chem. Soc.* **2013**, *135*, 6363–6371.
- (16) Yao, Z.; Zhang, M.; Wu, H.; Yang, L.; Li, R.; Wang, P. *J. Am. Chem. Soc.* **2015**, *137*, 3799–3802.
- (17) García, F.; Buendía, J.; Ghosh, S.; Ajayaghosh, A.; Sánchez, L. *Chem. Commun.* **2013**, *49*, 9278–9280.
- (18) Korevaar, P. A.; Schaefer, C.; de Greef, T. F. A.; Meijer, E. W. *J. Am. Chem. Soc.* **2012**, *134*, 13482–13491.
- (19) Jiang, W.; Qian, H.; Li, Y.; Wang, Z. *J. Org. Chem.* **2008**, *73*, 7369–7372.
- (20) Li, Y.; Wang, Z. *Org. Lett.* **2009**, *11*, 1385–1387.
- (21) (a) Prasanthkumar, S.; Saeki, A.; Seki, S.; Ajayaghosh, A. *J. Am. Chem. Soc.* **2010**, *132*, 8866–8867. (b) Malicka, J. M.; Sandeep, A.; Monti, F.; Bandini, E.; Gazzano, M.; Ranjith, C.; Praveen, V. K.; Ajayaghosh, A.; Armaroli, N. *Chem. - Eur. J.* **2013**, *19*, 12991–13001.
- (22) Kameta, N.; Masuda, M.; Minamikawa, H.; Shimizu, T. *Langmuir* **2007**, *23*, 4634–4641.
- (23) García, F.; Korevaar, P. A.; Verlee, A.; Meijer, E. W.; Palmans, A. R. A.; Sánchez, L. *Chem. Commun.* **2013**, *49*, 8674–8676.
- (24) Safont-Sempere, M. M.; Fernández, G.; Würthner, F. *Chem. Rev.* **2011**, *111*, 5784–5814.
- (25) Terashima, T.; Mes, T.; De Greef, T. F. A.; Gillissen, M. A. J.; Besenius, P.; Palmans, A. R. A.; Meijer, E. W. *J. Am. Chem. Soc.* **2011**, *133*, 4742.